Applied Catalysis B: Environmental 225 (2018) 445–451

Contents lists available at ScienceDirect

Applied Catalysis B: Environmental

journal homepage: www.elsevier.com/locate/apcatb

Photoelectrochemical synthesis of aniline from nitrobenzene in a neutral aqueous solution by using a *p*-type Cu_2ZnSnS_4 electrode

Sunao Kamimura[a,b,c,*], Yuki Kubo[a], Toshiki Tsubota[a], Teruhisa Ohno[a,c,d,*]

[a] Department of Applied Chemistry, Faculty of Engineering, Kyushu Institute of Technology, 1-1 Sensuicho, Tobata, Kitakyushu 804-8550, Japan
[b] PRESTO, Japan Science and Technology Agency, 4-1-8 Honcho, Kawaguchi-shi, Saitama 322-0012, Japan
[c] Research Center for Solar Light Energy Conversion, 1-1 Sensuicho, Tobata, Kitakyushu 804-8550, Japan
[d] ACT-C, Japan Science and Technology Agency, 4-1-8 Honcho, Kawaguchi-shi, Saitama 322-0012, Japan

ARTICLE INFO

Keywords:
Photoelectrochemistry
Photocathode
Cu_2ZnSnS_4
Photocatalyst
Nitrobenzene

ABSTRACT

We fabricated a CZTS electrode by the sol-gel and spin-coating method on an Mo/glass substrate and performed photoelectrochemical (PEC) reduction of nitrobenzene (NB) in an aqueous environment under visible light irradiation ($420 < \lambda < 800$ nm). By using the CZTS electrode, a six-electron reduction reaction of NB to aniline (AN) proceeded in an aqueous solution under visible light irradiation. We found that NB reduction reaction was strongly dependent on the electrode potential; large cathodic polarization is kinetically favorable for hydrogen evolution over a CZTS electrode, which leads to hindrance of the PEC NB reduction reaction, resulting in a decrease in the yield of AN (< 20%). At small cathodic polarization, conversion of NB reached to > 99% and the yield of AN was calculated to be > 50%. Moreover, we found that the proton concentration in an aqueous electrolyte had a significant effect on the PEC NB reduction reaction. In this study, we investigated the PEC NB reduction reaction over a CZTS electrode in conjunction with the structural and optical properties.

1. Introduction

Direct capture and storage of solar energy via the formation of chemical bonds, by analogy with natural photosynthesis, is a desirable alternate energy approach. One way to reach this goal is to directly convert water to H_2 and O_2 using a photoelectrode that has a photoresponse well matched to the solar spectrum [1–4]. PEC water splitting and CO_2 reduction has been extensively studied and it provides a viable energy resource with minimal environmental impact after combustion [5–10]. Recently, photoelectrochemical (PEC) organic synthesis based on the semiconductor-liquid junction has attracted much attention because it can proceed with a low electrical bias potential in contrast to electro-organic synthesis due to a part or all of the energy being supplied by incident light [11–15]. Moreover, it is possible to readily generate a wide variety of reactive products or intermediates by electron transfer at the electrode surface without the need for handling sensitive, expensive and toxic reagents. For example, Choi et al. reported a direct conversion of 5-hydroxymethylfurfural to 2,5-furandicarboxylic acid by using a $BiVO_4$ photoanode at an applied voltage far lower than the theoretical electrolysis voltage under visible light irradiation [16]. Wang and Domen et al. also succeeded in a direct conversion of toluene to methylcyclohexane by using a Pt/CdS/Cu_2ZnSnS_4 photocathode under visible light irradiation [17]. More recently, Tateno and Sayama et al. demonstrated PEC dimethoxylation of furan with methanol using a $BiVO_4/WO_3$ photoanode and Br^+/Br^- as a mediator with low applied potential [18].

We were inspired by their works and became interested in exploring the potential of PEC reduction of nitrobenzene (NB) to aniline (AN) using semiconductor photoelectrodes in an aqueous environment. AN is an important chemical substance that is widely used as a raw material in the production of methylene diphenyl diisocyanate, polyurethane, rubber and so on [19–21]. AN is currently manufactured by hydrogenation of nitrobenzene (NB), a process that is classified into two categories, namely batch process and continuous process [21]. The former category is called Bechamp reduction, an AN is generally obtained in 90–95% yield. However, removal of the spent iron catalyst when the manufacture is conducted on a large scale for AN presents a number of difficulties, both in handling and disposal. The latter category is further divided into vapor-phase catalytic hydrogenation and liquid-phase catalytic hydrogenation. The vapor-phase process quantitatively produces AN but needs special care due to the potentially explosive nature of H_2 gas and a relatively high temperature (473–573 K). The liquid-phase process has lower energy requirements than the vapor-phase process, but it requires product-catalyst separation. A new method that

* Corresponding authors at: Department of Applied Chemistry, Faculty of Engineering, Kyushu Institute of Technology, 1-1 Sensuicho, Tobata, Kitakyushu 804-8550, Japan
E-mail addresses: kamimura-sunao@che.kyutech.ac.jp (S. Kamimura), tohno@che.kyutech.ac.jp (T. Ohno).

https://doi.org/10.1016/j.apcatb.2017.12.021
Received 12 October 2017; Received in revised form 4 December 2017; Accepted 10 December 2017
Available online 11 December 2017
0926-3373/

produces AN from NB with mild reaction conditions is therefore desired.

For the reduction reaction of NB to AN in the presence of hydrogen, the thermodynamic requirement at 298 K is shown in Eq. (1),

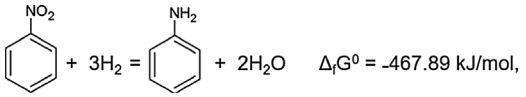

(1)

where Δ_fG^0 was estimated from standard formation enthalpies, Δ_fH^0, and standard molar entropies, S^0, in the database. This reaction free energy corresponds to $E^0 = 0.80$ V on the basis of a six-electron reaction as $\Delta_fG^0 = -nFE^0$, in which n and F are the number of electrons and the Faraday coefficient, respectively. The voltage required to drive the conversion of NB/AN is significantly less than that needed for conventional water splitting, 1.23 V. Thus, if NB can be reduced using water electrolyte as both an electron donor and a proton source, such a reaction could lead to preferential AN production in an aqueous solution. In addition, PEC NB reduction is considered to be an environment-friendly reaction system with advantages of a simple reaction system, no need for an organic solvent and easy product-catalyst separation.

In this study, we used the PEC system for direct conversion of NB to AN in an aqueous solution under visible light irradiation for the first time. Cu_2ZnSnS_4 (CZTS) was used as a photoelectrode in this study because of its ability to absorb visible light (band gap of ca. 1.5 eV) and it's *p*-type conductivity (photocathode) [22–26]. In addition, it is made of cheap, non-toxic, earth-abundant elements and can be easily produced on a large scale. Although hydrogen energy storage and CO_2 fixation have been studied by using a CZTS electrode, there has been no report on PEC conversion of NB to AN. In the present study, the PEC property for NB reduction was investigated in conjunction with the effects of an aqueous electrolyte. The PEC reaction process is also discussed.

2. Experimental section

2.1. Preparation of a Cu_2ZnSnS_4 electrode

The Cu_2ZnSnS_4 electrode was fabricated by the sol-gel and spin-coating method using the following procedure [25]. First, 0.4 mol/L Cu $(CH_3COO)_2{\cdot}H_2O$ (Wako, 99.0%), 0.25 mol/L $Zn(CH_3COO)_2{\cdot}2H_2O$ (Wako, 99.9%), 0.2 mol/L $SnCl_2{\cdot}2H_2O$ (Wako, 99.9%) and 1.6 mol/L $SC(NH_2)_2$ (Wako, 98%) were dissolved in 2-methoxyethanol (10 mL, Wako, 99.0%) containing monoethanolamine (Sigma-Aldrich, > 99.0%). The concentration of each metal ion coincides with the generally reported data for high-efficiency solar cells, and an excess amount of thiourea was used to complex metal ions and alleviate the loss of sulfur during the annealing process. To prevent the formation of cracks in the precursor thin film during the sulfurization process, additive monoethanolamine is necessary in the precursor solution. Approximately 70 μL of the precursor solution was dropped on an Mo-coated soda-lime glass (Mo/glass, 18 mm × 20 mm in size, GEOMATEC Co., Ltd.) and then the excess precursor solution was removed by spin-coating (3000 rpm, 30 s). The electrode was dried in air at 200 °C for 5 min on a hotplate. After this process had been repeated for a maximum of 5 times, the electrode was calcined at 560 °C for 1 h in a sulfur/N_2 atmosphere. To remove impurity phases such as $Cu_{2-x}S$ over the CZTS film, $(NH_4)_2S$ etching processes were performed for 6 h. Then a bare CZTS electrode was obtained.

2.2. Characterization

The crystalline phases were characterized by using a powder X-ray diffraction (XRD) instrument (MiniFlex II, Rigaku Co.) with CuKα (λ = 1.5418 Å) radiation (cathode voltage: 30 kV, current: 15 mA). Raman spectroscopy measurements were performed by using a JASCO NRS 5100 laser Raman spectrophotometer. Absorption properties of a CZTS electrode were determined by using the diffuse reflection method with a UV/VIS/NIR spectrometer (UV-2600, Shimadzu Co.) attached to an integral sphere at room temperature. X-ray photoelectron spectroscopy (XPS) measurements were performed by using a Kratos AXIS Nova spectrometer (Shimazu Co.) with a monochromatic Al Kα X-ray source. The binding energy was calibrated by taking the carbon (C) 1s peak of contaminant carbon as a reference at 284.6 eV. The wavelength dependence of incident photon to current efficiency (IPCE) was measured by using a Xe lamp equipped with a band-pass filter centered at 400 nm, 450 nm, 500 nm, 600 nm, 650 nm, and 700 nm, respectively (All band–pass filters were purchased from Asahi Spectra Co., Ltd., and full width at half maximum was 10 nm.). The IPCE at each irradiation wavelength was calculated by the following equation:

$$\text{IPCE}\ [\%] = 1240 \times J\ [\text{mA cm}^{-2}] \times 100/(\lambda\ [\text{nm}] \times I\ [\text{mW cm}^{-2}]),$$

where J is photocurrent density, λ is irradiation wavelength of the light-emitting diodes and I is irradiation intensity of incident light.

2.3. Photoelectrochemical (PEC) measurement

The PEC performance of the CZTS electrode was investigated in a three-electrode configuration using a silver–silver chloride (Ag/AgCl) reference electrode and a Pt coil counter electrode. The electrolyte was 0.1 M Eu^{3+}-containing aqueous solution. The electrolyte was purged with Ar gas for 30 min before PEC measurement. Linear sweep voltammetry and chronoamperometry measurements were carried out by using an automatic polarization system (HSV-110, Hokuto Denko Co.) under visible light irradiation (Xe lamp, 420 nm < λ < 800 nm, 100 mW/cm^2). The scan rate for the linear sweep voltammetry was 10 mV s^{-1}.

2.4. Analysis of products

PEC reduction of nitrobenzene to aniline was performed in a gas-tight three-electrode configuration cell with a double compartment in which a CZTS electrode, Pt coil and Ag/AgCl electrode were used as a working electrode, counter electrode and reference electrode, respectively. The working cell and counter cell were separated by Nafion membrane. The electrolyte solution was 0.1 M Na_2SO_4 with 100 μM NB. The pH was adjusted by using H_2SO_4 and NaOH aqueous solution. After Ar bubbling for 30 min, each cells were sealed and irradiated by visible light irradiation (Xe lamp, 420 nm < λ < 800 nm, 100 mW/cm^2). Evolved H_2 gas was detected by an on-line gas chromatograph (GC) with a thermal conductivity detector (MicroGC, Agilent Technology Co.) equipped with an MS-5A column. He gas was used as the carrier gas. Dissolved O_2 in aqueous electrolyte was estimated by using fiber-optic oxygen microsensors (FireSting, pyroscience). The products, AN, NB and NSB, were detected by high-performance liquid chromatography (CTO-10ASVP, Shimadzu) with an Inertsil ODS-2 column attached to a UV detector (SPD-20A). Conversion of NB, yield of AN, and selectivity for AN were defined as the follows:

$$\text{Conversion}(\%) = \left(\frac{C_0 - C_{NB}}{C_0}\right) \times 100,$$

$$\text{Yield}(\%) = \left(\frac{C_{AN}}{C_0}\right) \times 100,$$

$$\text{Selectivity}(\%) = \left(\frac{C_{AN}}{C_0 - C_{NB}}\right) \times 100,$$

where C_0 is the initial concentration of NB and C_{NB} and C_{AN} are concentrations of the substrate NB and corresponding AN at a certain time after the PEC reaction, respectively.

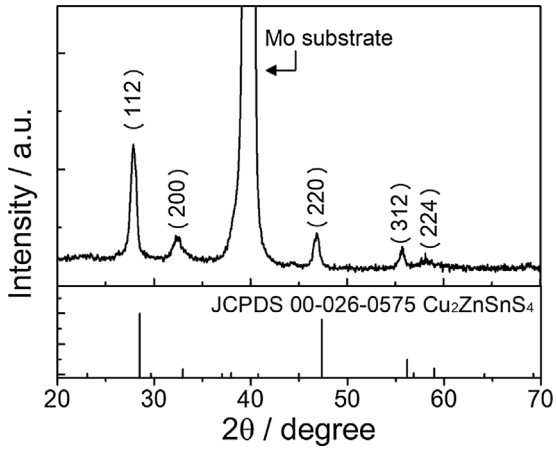

Fig. 1. XRD pattern of a Cu_2ZnSnS_4 electrode together with that of a reference pattern.

3. Results and discussion

Fig. 1 shows the XRD pattern of the CZTS electrode together with the ICDD standard file of the tetragonal phase of Cu_2ZnSnS_4 (JCPDS 00-026-0575). An intense peak corresponding to the bottom Mo substrate was observed at 40.02°, while other diffraction peaks coincided with the reference pattern corresponding to the (112), (200), (220), (312), (224) planes of CZTS. The results indicated that the polycrystalline CZTS film could be prepared by the sol-gel and spin-coating method. Raman scattering spectroscopy is a strong tool for determining impurity phases that cannot be identified effectively by XRD measurement. We therefore obtained the Raman spectrum of the CZTS electrode under 532 nm laser illumination (see Fig. 2). There is an intense peak centered at 325 cm^{-1} along with a weak peak located at 284 cm^{-1}; these signals are in agreement with those of the kesterite CZTS structure [25,26], and no other peaks were found to be binary phases such as hexagonal $Cu_{2-x}S$ (475 cm^{-1}), ZnS (353 cm^{-1}) and SnS (217 cm^{-1}) [26,27]. Raman peaks at 401 cm^{-1} indicate very thick MoS_2 covering on the Mo substrate [28]. Formation of the MoS_2 layer was inevitable in the sulfurization process of CZTS, which may facilitate electrical quasi-ohmic contact and improve the adhesion of CZTS to the Mo back contact but leads to high series resistance and accordingly deteriorates the device efficiency if the layers is not thin enough. In addition, SnO_2 phase as an impurity phase was observed at 647 cm^{-1} [27]. Thus, our fabricated CZTS electrode consists of the major phase of kesterite CZTS and minor phases of SnO_2.

Fig. 3 shows a cross-sectional SEM photograph of the CZTS electrode. The CZTS film with a flat and tight structure was observed to have good adhesion to the Mo substrate. The thickness of the CZTS layer was estimated to be ca. 400 nm. Moreover, an MoS_2 layer with a thickness of 60 nm was observed at the interface between the CZTS layer and Mo substrate.

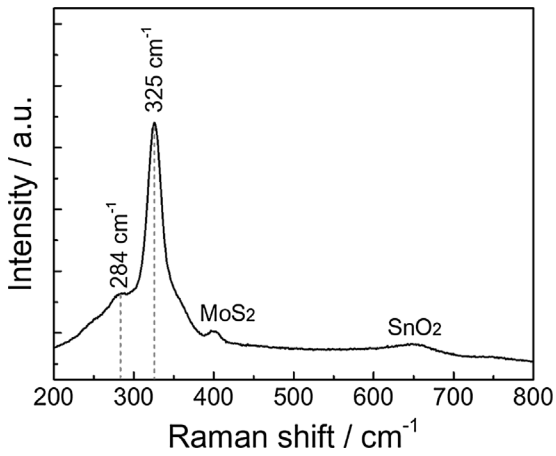

Fig. 2. Raman spectrum of a Cu_2ZnSnS_4 electrode under 532 nm laser illumination.

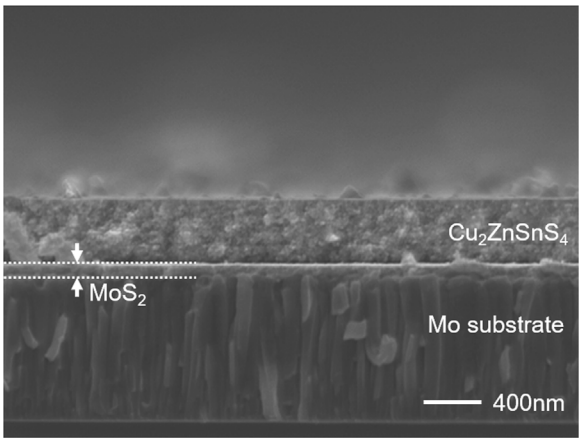

Fig. 3. Cross-sectional SEM photographs of the Cu_2ZnSnS_4 electrode.

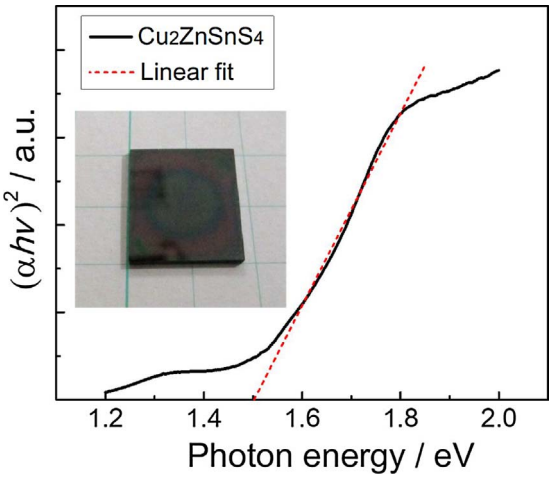

Fig. 4. Tauc plot for a CZTS electrode. The inset figure shows a picture of our fabricated CZTS electrode.

Fig. 4 shows the diffuse reflectance spectrum of the CZTS electrode. According to the results of theoretical calculation, CZTS is a direct energy gap material. The optical absorption of CZTS could be converted to a Tauc plot, $(\alpha h\nu)^n$ vs. $h\nu$, where n = 2 for a direct bandgap, by extending the tangential lines to the abscissa. The band gap of the CZTS electrode was estimated to be ca. 1.5 eV, which is consistent with the reported ones in references. [29]

For clarifying the flat band potential (V_{fb}) of CZTS, the current-potential characteristics were investigated by linear sweep voltammetry in the presence of $Eu(NO_3)_3$ as an electron scavenger (see Fig. 5). The pH was adjusted to 6.0 by using NaOH aqueous solution. A potential sweep was performed with a scan rate of 10 mV/sec under chopped illumination from a Xe lamp with cutoff filters ($420 < \lambda < 800$ nm). The CZTS electrode exhibited a cathodic photocurrent in response to irradiation of incident light, confirming that the prepared thin film was a *p*-type semiconductor. In bulk *p*-type semiconductor electrodes, photogenerated holes diffuse inside the semiconductor and can then be injected into a contacting metal electrode, unless the electrode potential is more positive than that of the flatband potential (V_{fb}) of the semiconductor. [30] Therefore, the potential of V_{fb} was assumed to be equal to the onset potential of the cathodic photocurrent. In this case, a cathodic photocurrent was observed at ca. +0.14 V vs. Ag/AgCl, suggesting that the potential of V_{fb} is +0.69 V vs. RHE for the CZTS electrode in the present electrolyte conditions. Moreover, in many

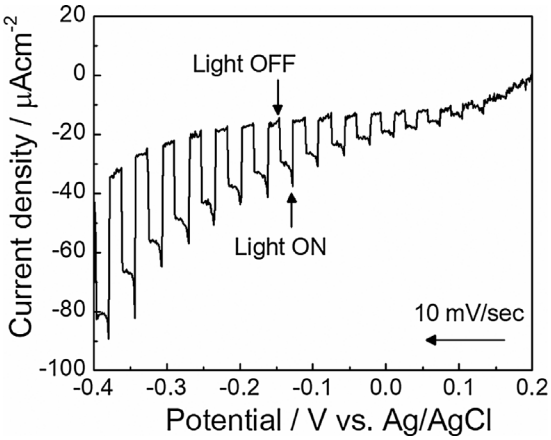

Fig. 5. Current-potential curve of a Cu_2ZnSnS_4 electrode in Eu^{3+} nitrate solution (pH 6, 100 mmol L^{-1}) under chopped illumination from a Xe lamp ($420 < \lambda < 800$ nm).

instances of *p*-type semiconductors, V_{fb} is comparable to the valence band maximum potential (VBM) of the corresponding semiconductors. Thus, the VBM and conduction band minimum (CBM) are considered to be located at ca. −0.81 V and +0.69 V vs. RHE, respectively. Our observations are consistent with a previous report [31].

We therefore carried out PEC NB reduction in a double-compartment three-electrode configuration cell using an Ag/AgCl reference electrode and a Pt coil counter electrode. Fig. 6a shows the current-potential curves of the CZTS electrodes in 0.1 M Na_2SO_4 electrolyte (pH 6.2) and 100 μM NB-containing Na_2SO_4 electrolyte solution under visible light irradiation ($420 < \lambda < 800$ nm). For the Na_2SO_4 electrolyte, onset potential for the cathodic photocurrent was ca. −0.1 V vs. Ag/AgCl. This value is more negative than that of the onset potential of the above CZTS system measured in an Eu^{3+} solution even though the measurement was carried out at the same pH. This may be because there is a significant potential barrier or a large number of surface defects that hinder electron transfer into water reduction reaction, similar to $CuInS_2$. Another possible reason is that there is a slow kinetics for water reduction reaction that results in electron accumulation on the surface of a CZTS electrode, and then subsequent surface recombination occurs until a sufficient applied potential is achieved for an appreciable charge transfer across the CZTS/electrolyte junction. However, no obvious difference between onset potential and V_{fb} was observed when 100 μM of NB was added to the Na_2SO_4 aqueous solution. Moreover, the photocurrent in the NB-containing Na_2SO_4 electrolyte was larger than that in the Na_2SO_4 electrolyte. Therefore, photogenerated electrons in the CBM of a CZTS electrode were consumed in the reduction of NB, the reaction being more preferential than the water reduction reaction. To clarify the irradiation wavelength dependence of the photocurrent of the CZTS electrodes in 0.1 M Na_2SO_4 electrolyte (pH 6.2) and 100 μM NB-containing Na_2SO_4 electrolyte solution, the action spectrum was acquired by determining the IPCEs at −0.4 V vs. Ag/AgCl as a function of the irradiation wavelength (see Fig. 6b). The IPCE obtained in 100 μM NB-containing Na_2SO_4 electrolyte was ca. 0.8% with irradiation wavelengths at 400 nm, which value was higher than that obtained in Na_2SO_4 electrolyte.

Fig. 7a shows the time course of the cathodic photocurrent from a CZTS electrode in NB-containing Na_2SO_4 solution at −0.4 V vs. Ag/AgCl under visible light irradiation ($420 < \lambda < 800$ nm) together with time courses of the amounts of NB and AN. The photocurrent gradually decreased with time, and it was decreased to ca. 99% of that in the initial state after 7 h of reaction. Importantly, the amount of NB also decreased with time and became negligibly low after 7 h of PEC reaction. These results implied that the decay behavior of the photocurrent was due to a decrease in the amount of NB in 0.1 M Na_2SO_4 solution. Furthermore, the amount of AN increased with an increase in irradiation time, followed by gradual saturation. After 7 h of PEC reaction, conversion of NB reached to > 99% and the yield of AN was calculated to be > 50%. These results indicated that PEC reduction of NB to AN could be achieved by using the CZTS electrode in an aqueous electrolyte. The mass balance was not matched before and after PEC reaction, as will be discussed later. It should be noted that the conversion of NB and the yield of AN was the best when 100 μM NB as the initial concentration was added to the aqueous electrolyte, as shown in Fig. 7b.

The CZTS electrode was stable after PEC reaction in the NB-containing Na_2SO_4 electrolyte. As shown in Fig. 8, there was almost no difference in the XPS spectra for Cu 2p, Zn 2p, Sn 3d and S 2p before and after PEC reactions for 7 h, indicating that the CZTS electrode is stable under PEC NB reduction reaction.

The dependence of the electrode potential on PEC NB reduction was investigated in the range between −0.4 V and −1.0 V vs. Ag/AgCl, and the results are shown in Fig. 9a. Product analysis was done after 1 h of PEC reaction. It should be noted that the products (H_2, NSB, and AN) were not detected either under dark conditions or under visible light irradiation in the absence of CZTS electrode. As can be seen in this figure, the amount of AN decreased with an increase of the cathodic polarization, and only a negligible amount of AN was produced at −1.0 V vs. Ag/AgCl. In contrast, an increase of H_2 evolution was observed with an increase of the cathodic polarization, suggesting that H_2 evolution competes with AN formation, lowering the FE for AN formation at a negative electrode potential [32]. In addition, NSB was observed through the PEC NB reduction reaction. In general, the reduction of NB is thought to occur via two pathways: hydroxylamine (direct) and azoxybenzene (indirect) pathways [33,34]. According to this mechanism, the direct pathway involves the reduction of NB to AN via NSB and hydroxylamine intermediates, whereas in the indirect pathway, NSB and hydroxylamine intermediates are condensed to form an azoxybenzene intermediate, which subsequently undergoes hydrogenation and cleavage of the azo bond to release aniline. Therefore, our results showing that NSB was obtained as an intermediate product of

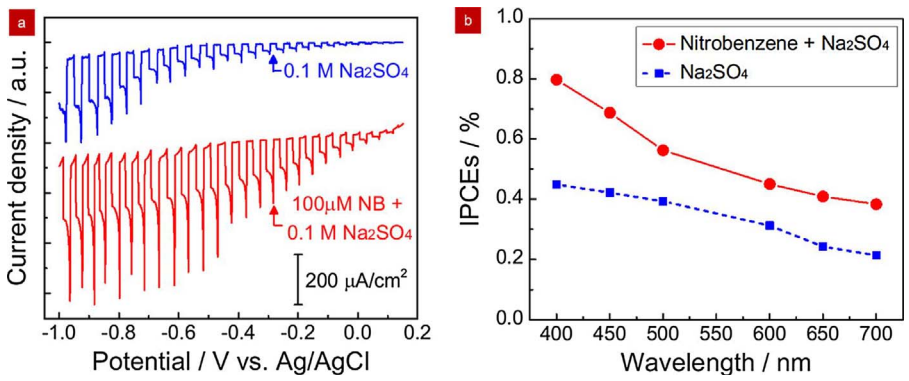

Fig. 6. (a) Current-potential curves of a CZTS electrode in 0.1 M Na_2SO_4 electrolyte (pH 6.2) with and without 100 μM NB under visible light irradiation ($420 < \lambda < 800$ nm). (b) The dependence of irradiation wavelengths on the photocurrent in 0.1 M Na_2SO_4 electrolyte (pH 6.2) with and without 100 μM NB.

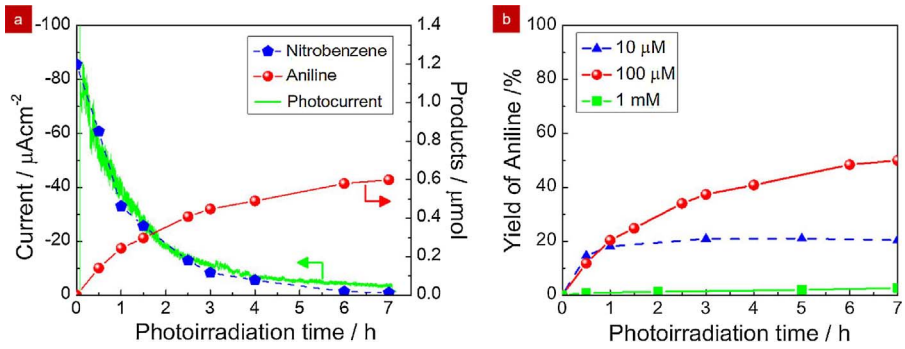

Fig. 7. (a) The left axis shows the time course of the photocurrent from a CZTS electrode in 100 μM NB-containing Na_2SO_4 electrolyte (pH 6.2) at −0.4 V vs. Ag/AgCl under visible light irradiation ($420 < \lambda < 800$ nm). The right axis shows the time course of the amounts of nitrobenzene and aniline under PEC reaction in an aqueous electrolyte. (b) Dependence of the initial concentration of NB on the yield of AN.

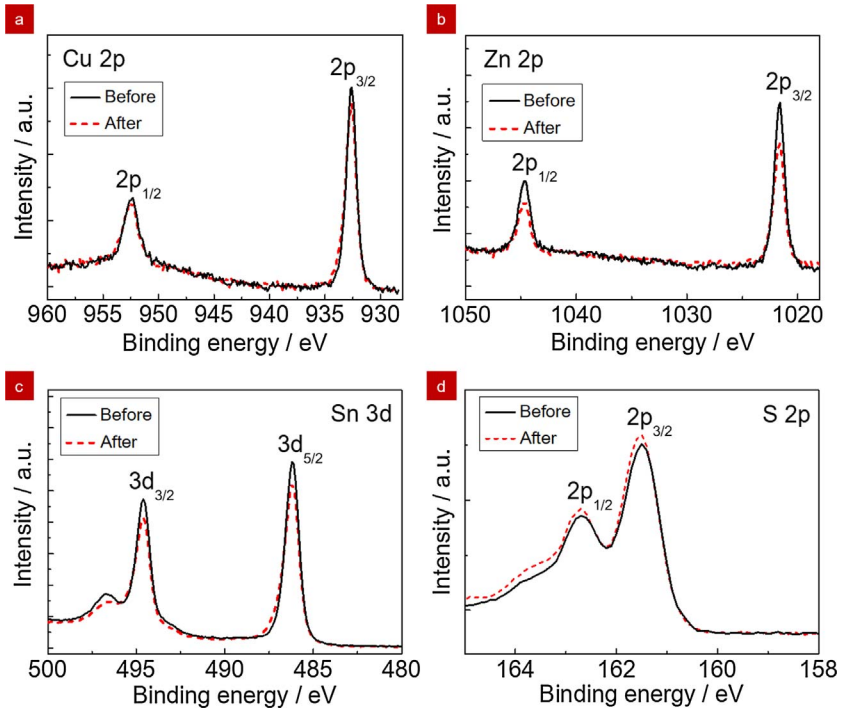

Fig. 8. XPS spectra for Cu 2p, Zn 2p, Sn 3d and S 2p before and after photoelectrochemical measurements of a CZTS electrode.

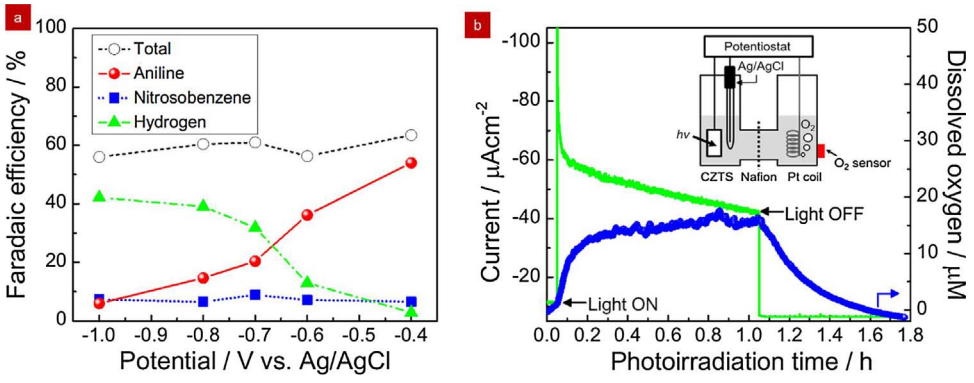

Fig. 9. (a) Photoelectrochemical reduction of NB over a Cu_2ZnSnS_4 electrode at different applied potentials ranging between −0.4 V and −1.0 V versus Ag/AgCl in 100 μM NB-containing Na_2SO_4 electrolyte (pH 6.2). (b) Time cource of the photocurrent of a CZTS electrode at −0.4 V versus Ag/AgCl, together with that of dissolved O_2 in 100 μM NB-containing Na_2SO_4 electrolyte (pH 6.2).

NB reduction reaction are reasonable. In addition, other intermediates such as phenylhydroxylamine and azoxybenzene were detected by high-performance liquid chromatography; however, quantitative analysis was not possible because these compounds were unstable in an aqueous environment at room temperature. As shown in Fig. 9b, O_2 evolution was confirmed as an anodic reaction. Since accurate quantification of evolved O_2 gas was difficult in this study due to its poor photocurrent density, we measured dissolved oxygen in aqueous electrolyte by fiber-optic oxygen microsensors. Amount of dissolved oxygen in 0.1 M Na_2SO_4 solution was increased as an increase of photoirradiation time, indicating that water oxidation reaction was occurred at counter electrode (Pt coil). Therefore, PEC NB reduction to AN is a good candidate as a new artificial photosynthesis.

Many reports suggest that NB reduction reaction goes through the direct or indirect pathway or via both the intermediates. In any case, H^+ (or H_2) addition is necessary in the NB reduction. We therefore studied the effect of H^+ concentration on PEC NB reduction over a CZTS electrode. Fig. 10 shows current-potential curves of CZTS

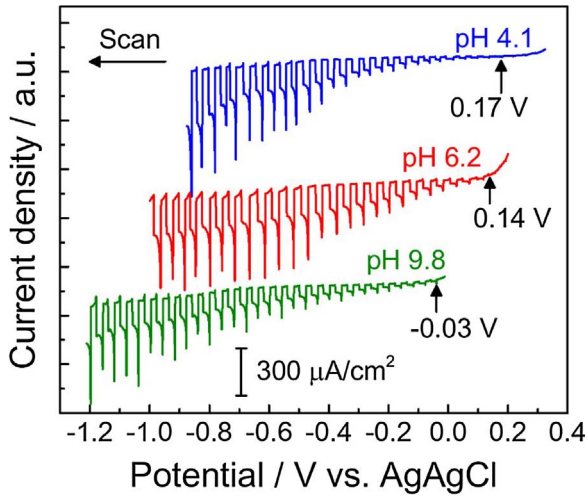

Fig. 10. Current-potential curves of a CZTS electrode in 100 μM NB-containing Na_2SO_4 electrolyte with different pH values under visible light irradiation (420 < λ < 800 nm).

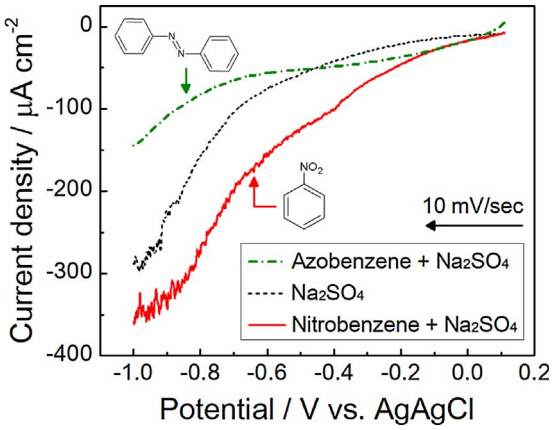

Fig. 12. Current-potential curves of a CZTS electrode in 0.1 M Na_2SO_4 electrolyte, 10 μM azobenzene-containing Na_2SO_4 electrolyte and 100 μM NB-containing Na_2SO_4 electrolyte under visible light irradiation (420 < λ < 800 nm).

electrodes in 100 μM NB-containing aqueous 0.1 M Na_2SO_4 solutions with different pH conditions (pH 4.1, 6.2, 9.8). The pH of the Na_2SO_4 solution was adjusted by using H_2SO_4 or NaOH aqueous solution. A cathodic photocurrent was observed from all of the solutions, and the photocurrent in the range between +0.1 and −0.7 V vs. AgAgCl in pH 6.2 neutral solution was larger than that in other solutions. Moreover, by considering that the band position of chalcogenide does not change with change in pH, these results implied that the surface conditions (e.g., adsorption of NB and an intermediate) of a CZTS electrode are favorable for NB reduction at pH 6.2.

Fig. 11a–c shows time courses of the amounts of NB, NSB and AN over a CZTS electrode at different pH conditions under visible light irradiation. It should be noted that the electrode potential was kept at −0.4 V vs. Ag/AgCl. In an acidic solution at pH 4.1, the conversion of

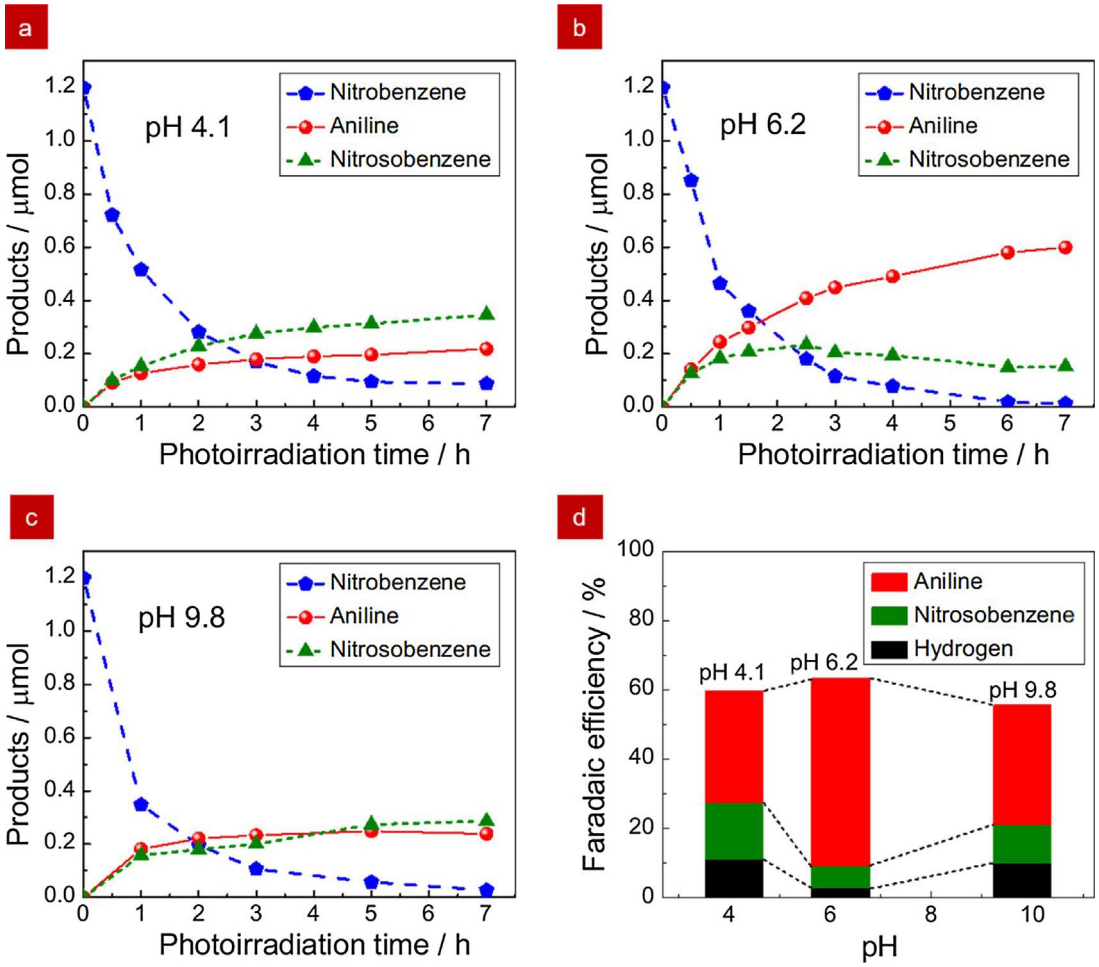

Fig. 11. Time courses of the amounts of NB, NSB and AN under PEC reaction in different pH solution: (a) pH 4.1, (b) pH 9.8, and (c) pH 6.2. (d) Product analysis after 1 h of PEC reaction in different pH solution.

NB and the yield of AN after 7 h of PEC reaction were 92% and 18%, respectively. A two-proton reduction reaction of NB to NSB was dominant in pH 4.1 solution. This may be because acidic conditions are kinetically favorable for hydrogen evolution since H^+ is abundant in the solution. Indeed, H_2 evolution at -0.4 V vs. Ag/AgCl in an acidic solution at pH 4.1 was larger than that in a neutral solution at pH 6.2 (see Fig. 11d). Another possible reason is that H_2 evolution caused a decrease in the H^+ concentration (an increase in the OH^- concentration) around a CZTS electrode, and the resulting gradient in the concentration interfered with NB reduction. In a basic solution at pH 9.8, the conversion of NB and the yield of AN after 7 h of PEC reaction were 98% and 20%, respectively (see Fig. 11b). This is thought to be caused mainly by slow kinetics for proton addition reaction that results in electron accumulation on the surface of a CZTS electrode, leading to hindrance of six-electron reductions (AN production) coupled with six protons, and then subsequent surface recombination occurs or two-electron reduction reaction (H_2 evolution) preferentially occurs. In a neutral solution at pH 6.2, the conversion of NB and the yield of AN after 7 h of PEC reaction were 99% and 50%, respectively (see Fig. 11c). Thus, AN production in pH 6.2 solution was greater than that in other solutions, indicating that neutral aqueous electrolyte with the lowest total concentration of H^+ and OH^-, was the most effective condition for PEC NB reduction to AN over a CZTS electrode because competition reaction including H_2 evolution was suppressed. As shown in Fig. 11a–c, a mass balance was not matched in spite of prolonged PEC reaction. In the ideal case, the total amount of organic carbons should be the same value before and after the reaction. This discrepancy is considered to be caused by a large overpotential for the reduction of the intermediates such as phenylhydroxylamine and azobenzene. This finding was confirmed by testing current-potential curves in the intermediates-containing electrolytes. As shown in Fig. 12, the onset potential observed in azobenzene-containing electrolyte was shifted toward negative potential comparing with that obtained in NB-containing electrolyte. Thus, a CZTS electrode exhibits a large overpotential for the reduction of azobenzene, which leads to an inhibition of AN production. If the electrode potential is shifted toward negative potential for the reduction of an intermediate, the AN production competes with H_2 evolution, resulting in a low yield of AN. Thus, PEC NB reduction reaction in aqueous electrolyte is a complicate reaction process in conjunction with proton reduction reaction. Although we demonstrated for the first time the PEC synthesis of AN from nitrobenzene in an aqueous electrolyte, other aspects such as the reaction pathway (direct or indirect pathway) are not yet clear. Further research is required to understand the PEC NB reduction process.

4. Conclusions

PEC production of AN from NB in an aqueous electrolyte was successfully demonstrated in a PEC cell consisting of a CZTS photocathode with advantages of good chemical stability, suitable band gap for the solar spectrum, the no toxicity and low cost. We reported that NB reduction reaction was strongly dependent on the electrode potential: preferential AN production in an aqueous solution occurred at a small cathodic polarization, while H_2 evolution competed with AN production reaction at a large cathodic polarization. Furthermore, we revealed that the yield of AN was strongly dependent on pH of the aqueous electrolyte; an acidic condition (pH 4.1) are kinetically favorable for hydrogen evolution over a CZTS electrode, which leads to hindrance of the PEC NB reduction reaction, resulting in a decrease in the yield of AN ($< 18\%$). Basic conditions (pH 9.8) are slow kinetics for proton addition reaction that results in electron accumulation on the surface of a CZTS electrode, which leads to inhabitation of six-proton reduction reaction, resulting in a decrease in the yield of AN ($< 20\%$). Therefore, PEC NB reduction reaction could not proceeded in an acidic or basic solution because H_2 evolution competed with AN production or proton addition reaction was limited. We found that PEC NB reduction to AN is occurred efficiency in a neutral aqueous electrolyte (pH 6.2) with the yield of AN reaching 50%. Thus, we revealed that a CZTS electrode has sufficient potential for facilitating a six-electron reduction reaction with six protons in an aqueous solution. The results of this could be applied to other organic compounds and would be helpful for the study of multi-electron reduction reaction of PEC reaction.

Acknowledgements

The authors thank Mr. Yousuke Sasaki and Mr. Masaki Kanaya for their valuable contributions to this study. This research was supported by the PRESTO program (Grant Number JPMJPR16P4) from Japan Science and Technology Agency (JST), a Grant-in-Aid for Young Scientists (B) (16K17895) and Advanced Catalytic Transformation program for Carbon utilization (ACT−C Grant Number JPMJCR12Y5).

References

[1] T. Hisatomi, J. Kubota, K. Domen, Chem. Soc. Rev. 43 (2014) 7520–7535.
[2] R. Abe, M. Higashi, K. Domen, J. Am. Chem. Soc. 132 (2010) 11828–11829.
[3] S. Ida, K. Yamada, T. Matsunaga, H. Hagiwara, Y. Matsumoto, T. Ishihara, J. Am. Chem. Soc. 132 (2010) 17343–17345.
[4] A. Paracchino, V. Laporte, K. Sivula, M. Grätzel, E. Thimsen, Nat. Mater. 10 (2011) 456–461.
[5] M. Higashi, K. Domen, R. Abe, Energy Environ. Sci. 4 (2011) 4138–4147.
[6] S. Sato, T. Arai, T. Morikawa, K. Uemura, T.M. Suzuki, H. Tanaka, T. Kajino, J. Am. Chem. Soc. 133 (2011) 15240–15243.
[7] S. Arai, S. Tajima, K. Sato, T. Uemura, T. Morikawa, T. Kajino, Chem. Commun. 47 (2011) 12664–12666.
[8] F. Jiang, T. Gunawan, Y. Harada, T. Kuang, K. Minegishi, K. Domen, S. Ikeda, J. Am. Chem. Soc. 137 (2015) 13691–13697.
[9] S. Kamimura, M. Higashi, R. Abe, T. Ohno, J. Mater. Chem. A 4 (2016) 6116–6123.
[10] S. Kamimura, N. Beppu, Y. Sasaki, T. Tsubota, T. Ohno, J. Mater. Chem. A 5 (2017) 10450–10456.
[11] V. Kalousek, P. Wang, T. Minegishi, T. Hisatomi, K. Nakagawa, S. Oshima, Y. Kobori, J. Kubota, K. Domen, ChemSusChem 7 (2014) 2690–2694.
[12] L. Bai, F. Li, Y. Wang, H. Li, X. Jiang, L. Suna, Chem. Commun. 52 (2016) 9711–9714.
[13] Y. Kageshima, T. Minegishi, T. Hisatomi, T. Takata, J. Kubota, K. Domen, ChemSusChem 10 (2017) 659–663.
[14] H. Tateno, Y. Miseki, K. Sayama, ChemElectroChem 4 (2017) 1–6.
[15] T. Li, T. Kasahara, J. He, K.E. Dettelbach, G.M. Sammis, C.P. Berlinguette, Nat. Commun 8 (2017) 390.
[16] H.G. Cha, K.-S. Choi, Nat. Chem. 7 (2015) 328–333.
[17] P. Wang, T. Minegishi, G. Ma, K. Takanabe, Y. Satou, S. Maekawa, Y. Kobori, J. Kubota, K. Domen, J. Am. Chem. Soc. 134 (2012) 2469–2472.
[18] H. Tateno, Y. Miseki, K. Sayama, Chem. Commun. 53 (2017) 4378–4381.
[19] J. Wang, Z. Yuan, R. Nie, Z. Hou, X. Zheng, Ind. Eng. Chem. Res. 49 (2010) 4664–4669.
[20] A. Corma, P. Concepci, P. Serna, Angew. Chem. Int. Ed. 46 (2007) 7266–7269.
[21] S. Travis, Z. Rappoport (Ed.), The Chemistry of Anilines, John Wiley & Sons, Ltd., Chichester, UK, 2007.
[22] D. Yokoyama, T. Minegishi, K. Jimbo, T. Hisatomi, G. Ma, M. Katayama, J. Kubota, H. Katagiri, K. Domen, Appl. Phys. Express 3 (2011) 101202.
[23] L. Rovelli, S.D. Tilley, K. Sivula, ACS Appl. Mater. Interfaces 5 (2013) 8018–8024.
[24] F. Jiang, T. Gunawan, Y. Harada, T. Kuang, K. Minegishi, K. Domen, S. Ikeda, J. Am. Chem. Soc. 137 (2015) 13691–13697.
[25] S. Kamimura, Y. Sasaki, M. Kanaya, T. Tsubota, T. Ohno, RSC Adv. 6 (2016) 112594–112601.
[26] Z. Su, K. Sun, Z. Han, H. Cui, F. Liu, Y. Lai, J. Li, X. Hao, Y. Liu, M.A. Green, J. Mater. Chem. A 2 (2014) 500–509.
[27] M. Grossberg, J. Krustok, J. Raudoja, K. Timmo, M. Altosaar, T. Raadik, Thin Solid Films 519 (2011) 7403–7406.
[28] F. Liu, K. Sun, W. Li, C. Yan, H. Cui, L. Jiang, X. Hao, M.A. Green, Appl. Phys. Lett. 104 (2014) 051105.
[29] N. Guijarro, M.S. Prévot, K. Sivula, J. Phys. Chem. Lett. 5 (2014) 3902–3908.
[30] T. Kameyama, T. Osaki, K. Okazaki, T. Shibayama, A. Kudo, S. Kuwabata, T. Torimoto, J. Mater. Chem. 20 (2010) 5319–5324.
[31] S. Huang, W. Luo, Z. Zou, J. Phys. D: Appl. Phys. 46 (2013) 235108.
[32] J.J. Roylance, T.W. Kim, K.-S. Choi, ACS Catal. 6 (2016) 1840–1847.
[33] A. Mahata, R.K. Rai, I. Choudhuri, S.K. Singh, B. Pathak, Phys. Chem. Chem. Phys. 16 (2014) 26365–26374.
[34] X. Dai, M. Xie, S. Meng, X. Fu, S. Chen, Appl. Catal. B: Environ. 158–159 (2014) 382–390.